Research Square

Preprints are preliminary reports that have not undergone peer review.
They should not be considered conclusive, used to inform clinical practice,
or referenced by the media as validated information.

Sleep Deprivation Activates Spinal Microglia via MitoROS Mediated mtDNA-cGAS- STING Signaling to Promote Postoperative Hyperalgesia

Hongqin Tu
Nanjing University
Xianjing Si
Nanjing University
Meilin Chu
Dalian Medical University
Rui Xu
Nanjing University
Yulin Huang
Nanjing University
Wei Zhang
Nanjing University
Xiaoping Gu
xiaopinggu@nju.edu.cn
Nanjing University

Research Article

Keywords: Sleep deprivation, Chronic postsurgical pain, Mitochondrial oxidative stress, Mitochondrial damage, cGAS-STING, Spinal microglia

Posted Date: November 9th, 2026

DOI: https://doi.org/10.21203/rs.3.rs-11108570/v1

License: This work is licensed under a Creative Commons Attribution 4.0 International License.
Read Full License

Additional Declarations: No competing interests reported.

Sleep Deprivation Activates Spinal Microglia via MitoROS Mediated mtDNA-cGAS-STING Signaling to Promote Postoperative Hyperalgesia

Hongqin Tu[1†], Xianjing Si[1†], Meilin Chu[2], Rui Xu[1], Yulin Huang[1*], Wei Zhang[1,2*], Xiaoping Gu[1*]

[1]Department of Anesthesiology, Nanjing Drum Tower Hospital, Affiliated Hospital of Medical School, Nanjing University, Nanjing, China.

[2]Dalian Medical University, Dalian, Liaoning 116044, China.

[†]Hongqin Tu and Xianjing Si contributed equally to this article.

*Correspondence:

Yulin Huang

hyl199006@126.com;

Wei Zhang

zhangwei2008@njmu.edu.cn;

Xiaoping Gu

xiaopinggu@nju.edu.cn

Abstract

Background: Sleep deprivation (SD) is a major risk factor for the chronification of postoperative pain, yet the underlying mechanisms remain poorly understood. Emerging evidence indicates that mitochondrial dysfunction and innate immune signaling may contribute to central sensitization and persistent pain.

Methods: We used a mouse model combining 48-hour SD with plantar incision (SD+I) to investigate the mechanisms linking SD to postoperative hyperalgesia. Mechanical pain sensitivity was assessed behaviorally, while spinal microglial activation, proinflammatory cytokine expression (IL-1β, IL-6, TNF-α), and mitochondrial function including structure, membrane potential, ATP production, and mitochondrial reactive oxygen species (MitoROS) levels were evaluated. The involvement of the mtDNA-cGAS-STING pathway was assessed using pharmacological interventions with the mitochondria-targeted antioxidant Mito-Tempo and the STING inhibitor C-176.

Results: SD significantly prolonged postoperative mechanical hyperalgesia and enhanced spinal microglial activation, accompanied by elevated IL-1β, IL-6, and TNF-α expression. SD+I mice exhibited mitochondrial structural damage, decreased membrane potential and ATP production, and excessive MitoROS accumulation. This mitochondrial stress caused the release of mtDNA into the cytosol, thereby activating the cGAS-STING signaling pathway. Treatment with Mito-Tempo or C-176 effectively suppressed microglial activation, reduced neuroinflammatory cytokine production, and alleviated postoperative hyperalgesia.

Conclusions： Mitochondrial oxidative stress plays a crucial role in sleep deprivation-induced postoperative hyperalgesia, excessive activation of which promotes mtDNA-cGAS-STING-mediated spinal microglial activation and prolonged hyperalgesia. The reversal of neuroinflammation and pain hypersensitivity by Mito-Tempo or C-176 emphasizes the mechanistic and therapeutic relevance of this pathway for preventing sleep deprivation-related postoperative hyperalgesia.

Keywords: Sleep deprivation; Chronic postsurgical pain; Mitochondrial oxidative stress; Mitochondrial damage; cGAS-STING; Spinal microglia;

2.Introduction

Chronic postsurgical pain (CPSP) is a common and debilitating complication after surgery. Sleep disturbances are also highly prevalent in the perioperative period, and accumulating evidence suggests a high comorbidity between sleep disturbances and CPSP[1]. A large-scale clinical cohort study reported that poor preoperative sleep quality is a reliable predictor of chronic pain following total knee arthroplasty and other major surgeries[2]. Despite increasing clinical awareness, the underlying neurobiological mechanisms linking sleep disturbances to CPSP remain incompletely understood.

Microglia, the resident immune cells of the central nervous system, are key regulators of pain processing[3]. In neuropathic pain, microglial activation induces the release of neuroinflammatory mediators that engage various cascading pathways including p38MAPK, NF-κB, and Nrf2/HO-1, thereby shifting the balance between pro- and anti-inflammatory cytokines to modulate pain sensitivity[4]. Recent studies suggest that activated spinal microglia are critically involved in the sleep deprivation-induced transition from acute to chronic pain[5, 6]. However, the early triggers driving this aberrant spinal microglial activation and subsequent neuroinflammation remain unclear.

Mitochondria are essential for energy metabolism and redox homeostasis, and dysfunction of mitochondria in glial cells and neurons has been linked to chronic pain[7-9]. Moreover, we previously observed spinal ROS accumulation in the mouse model of sleep deprivation with incisional pain, and intrathecal administration of the ROS scavenger phenyl-N-tert-butylnitrone (PBN) significantly inhibited spinal microglial activation and inflammasome activity[10]. Given that MitoROS, a primary source of intracellular ROS, can surge dramatically in response to pathogens and damage signals, causing oxidative damage to mitochondrial proteins, lipids, and DNA[11]. We hypothesize that MitoROS serves as the initial trigger mediating mitochondrial damage and driving spinal microglial activation in sleep deprivation-induced chronic postoperative pain.

Notably, mtDNA is particularly vulnerable to MitoROS attack due to its proximity to the respiratory chain and lack of histone protection [12]. Cytosolic mtDNA functions as

a mitochondrial damage-associated molecular pattern (mtDAMP) that activates pattern recognition receptors (PRRs)[13]. Among these, cGAS was found highly expressed in microglia[14]. Upon binding to double-stranded DNA, cGAS catalyzes the production of the second messenger cyclic GMP-AMP (cGAMP), thereby activating the STING signaling pathway and triggering downstream inflammatory signaling[15].

Here, we sought to explore the relationship among MitoROS, mitochondrial dysfunction, and the cGAS-STING pathway in spinal microglia, and their contribution to sleep deprivation-induced chronic postsurgical pain. To this end, we used a mouse model combining continuous sleep deprivation and plantar incision to examine mitochondrial dysfunction, MitoROS levels, cytosolic mtDNA accumulation, microglial activation, and GAS-STING pathway expression. We further evaluated whether pharmacological clearance of MitoROS with Mito-Tempo could restore mitochondrial function and attenuate microglial activation, and evaluated the therapeutic effects of Mito-Tempo and the STING-specific inhibitor C-176 on sleep deprivation-induced postoperative hyperalgesia.

3.Materials and Methods

3.1 Animals

Adult male C57BL/6J mice with 8 weeks old purchased from Beijing Vital River Laboratory Animal Technology (Beijing, China). They were housed under controlled environmental conditions at 21±1°C with 50±5% relative humidity and a 12-h light/dark cycle (lights on at 8:00 am). Food and water were available ad libitum throughout the study. All experimental procedures were conducted after at least 1 week of acclimatization.

3.2 Model of Sleep Deprivation

Sleep deprivation was performed using an automated sleep deprivation apparatus (XR-XS108, Xinruan, Shanghai). The device induces tactile stimulation through the rotation of an interfering rod at the chamber base, with randomized directional reversals to prevent habituation and ensure sustained wakefulness in mice. Briefly, we put the mice into the cylinder to adapt for 30min, initiated the SD procedure, programming the apparatus to deliver intermittent rotational stimulation (7 rpm, 15-second duration per cycle) continuously for 48 hours.

3.3 Model of Plantar incision

Following Brennan's method[16], a plantar incision model was established to simulate postoperative pain. Briefly, mice were anesthetized via sevoflurane inhalation administered through a nasal mask. The plantar skin of the right hind paw was disinfected with 10% povidone-iodine solution, followed by a 0.5~1 cm midline longitudinal incision through the skin and subcutaneous tissue to expose the underlying muscle. The flexor digitorum brevis muscle was gently elevated with curved forceps inserted beneath its lateral edge and advanced medially, taking care to avoid nerve injury. After hemostasis was achieved by gentle pressure, the skin was closed with 5-0 nylon sutures.

3.4 50% Paw Withdrawal Threshold Test for Pain Assessment

Mice were firstly acclimated for 30 minutes in individual transparent plexiglass chambers positioned on an elevated wire mesh platform. The 50% mechanical paw withdrawal threshold was assessed using calibrated von Frey filaments (North Coast, USA) according to the up-down method [17]. The test began with the application of a 0.6 g filament to the mid-plantar surface of the right hindpaw, the filament was applied perpendicularly and held for 4~6 seconds. A positive response was defined as a rapid paw withdrawal, licking, or shaking of the stimulated paw. In the absence of a response, the next filament of higher force (1.0 g) was applied; if a response occurred, a filament of lower force (0.4 g) was used in the subsequent trial. Stimuli were delivered at intervals of at least 30 seconds to avoid sensitization. After the first positive response, four additional measurements were collected, after which the up-down sequence was terminated and the 50% paw withdrawal threshold was calculated based on the response pattern, using filament forces ranging from 0.07g to 2.0g.

3.5 Drug Administration

The selective STING inhibitor C-176 (HY-112926, MedChemExpress) and the mitochondrial-targeted antioxidant Mito-Tempo (HY-112879, MedChemExpress) were initially prepared as concentrated stock solutions in dimethyl sulfoxide (DMSO)and then diluted to the desired working concentrations with 0.9% saline immediately before administration. Mice subjected to the combined sleep deprivation and plantar incision model were randomly assigned to receive daily intraperitoneal injections (i.p.) of either C-176 (200 μl, 5 mg/kg) or Mito-Tempo (200 μl, 1.4 mg/kg), whereas control animals received equivalent volumes of 0.9% saline with corresponding DMSO carrier. All treatments were administered once daily beginning 24 hours before the onset of sleep deprivation and continuing through postoperative day 14. The chosen dose regimens and administration routes were based on prior in vivo studies demonstrating effective suppression of STING activation and mitochondrial oxidative stress without overt

toxicity[18, 19].

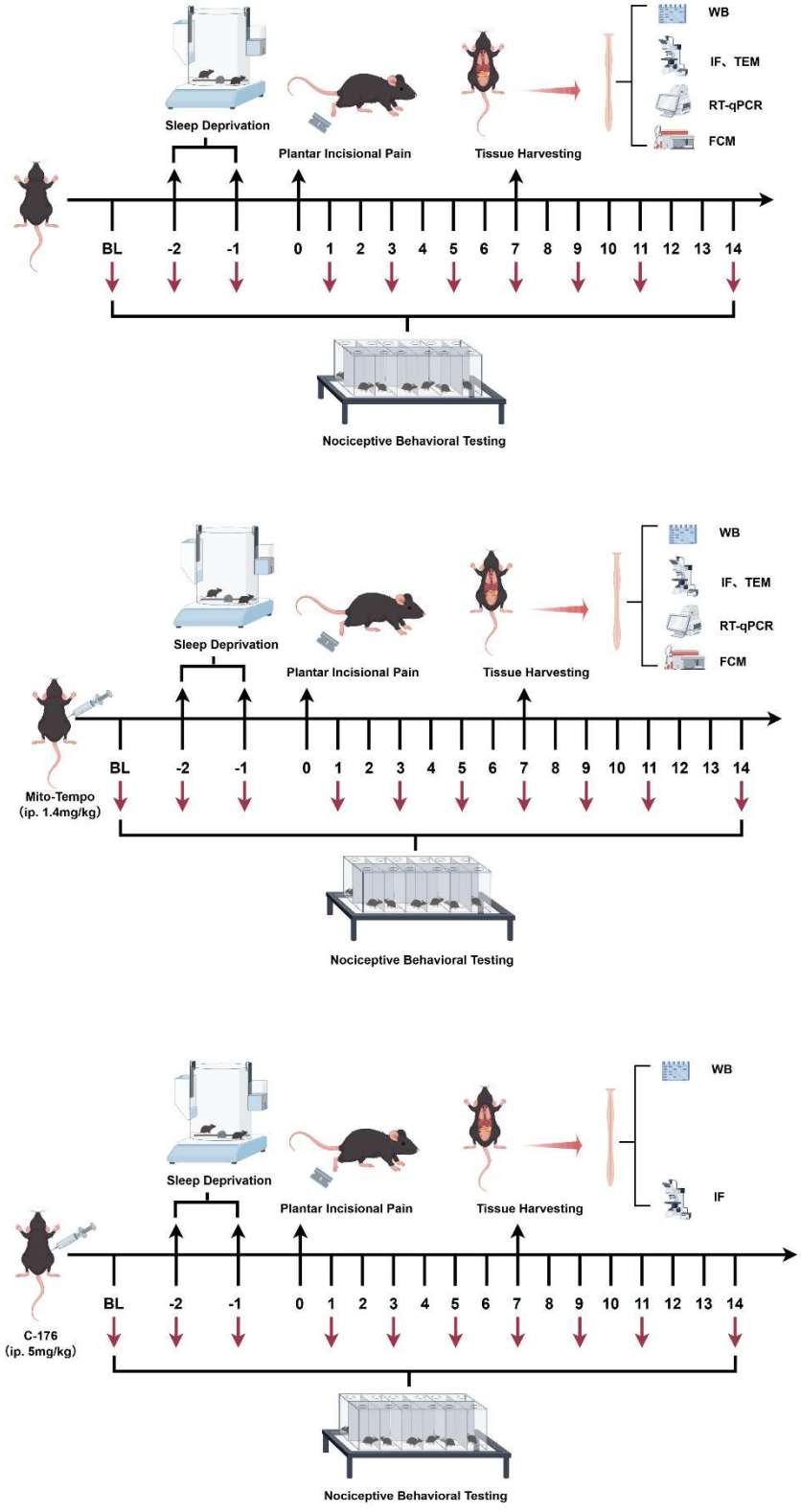


Fig1. Experimental designs and animal groups

3.6 Western blot

The spinal cord was rapidly removed from mice under deep anesthesia and homogenized in ice-cold tris lysis buffer supplemented with protease inhibitor cocktail and phosphatase inhibitors. The homogenate was centrifuged at 12,000 rpm at 4 ˚C for 15min and the supernatant was collected. Protein concentration was quantified using a BCA Protein Assay Kit (P0010, Beyotime, China). Equal amounts of protein (20 μg per sample) were separated by SDS-PAGE (PG-112, Epizyme Biotech, China) and transferred onto transferred onto polyvinylidene fluoride (PVDF) membranes (IPVH00010, Millipore, USA) at 300 mA for 90 min. The membranes were blocked with 5% skim milk for 1 h at room temperature, followed by overnight incubation at 4°C with the corresponding primary antibodies diluted with Tris-buffered saline containing 0.1% Tween-20 (TBST). After three washes with TBST, the membranes were incubated with HRP-conjugated secondary antibodies for 2 h at RT. Protein bands were detected using ECL Prime Detection Reagent (E412-02, Vazyme, China) and imaged with a Tanon-4600 Chemiluminescent Imaging System (Tanon, China). Target protein expression was quantified using ImageJ software (NIH, Bethesda, MD, USA). The antibodies used are listed in Table 1.

Table 1

The detailed information on antibodies.

Antibodies	Source	Identifier	Dilution	Applications
IL-1β	Cell Signaling Technology	Cat #12703	1:1000	WB
IL-6	Cell Signaling Technology	Cat #12912	1:1000	WB
TNF-α	Abcam	Cat #ab183218	1:500	WB
STING Pathway Antibodies	Cell Signaling Technology	Cat #16029	1:1000	WB
GAPDH	Affinity	Cat #T0004	1:10000	WB
Iba1	Abcam	Cat #ab178846	1:1000	IF
STING	Merck	Cat #MABF270	1:150	IF

HRP-labeled Goat Anti-Rabbit IgG(H+L)	Beyotime	Cat #A0216	1:1000	WB
HRP-labeled Goat Anti-Mouse IgG(H+L)	Beyotime	Cat #A0208	1:1000	WB
Alexa Fluor 488-labeled goat anti-rabbit secondary antibody	Invitrogen-Thermo Fisher Scientific	Cat #A32731	1:1000	IF
Alexa Fluor 647-labeled goat anti-rabbit secondary antibody	Invitrogen-Thermo Fisher Scientific	Cat #A32733	1:1000	IF

3.7 Immunofluorescence staining

Under deep anesthesia, mice were intracardially perfused with phosphate-buffered saline (PBS) followed by 4% paraformaldehyde (PFA). The L3-L5 spinal cord segments were dissected, fixed overnight in 4% PFA, and cryoprotected in 30% sucrose at 4°C, and sectioned at 25 μm using a cryostat (CM1900, Leica, Wetzlar, Germany). After three washes with PBS, sections were blocked with 0.1% Triton X-100 and 2% BSA for 2 h at RT, incubated overnight with primary antibodies at 4°C, and then with fluorophore-conjugated secondary antibodies for 2 h at room temperature after PBS washes. Images were acquired using a fluorescence microscope (Leica Microsystems, Wetzlar, Germany), and mean fluorescence intensity and colocalization were analyzed using ImageJ with the JACoB plugin. Antibodies are also listed in Table 1.

3.8 Microglia isolation via Magnetic-activated cell-sorting (MACS)

To assess mitochondrial functional status in microglia isolated from mouse spinal cord tissue, $CD11b^+$ cells were purified using MACS technology. Firstly, the spinal cord freshly dissociated from mice were immediately digested in enzymatic dissociation buffer for 30min at RT. The resulting tissue homogenate was passed through a 70-μm cell strainer to obtain a single-cell suspension. After washing with PBS, the cells were

incubated with anti-CD11b microbeads (Miltenyi Biotec, 130-049-601, Germany) for 15 min at 4°C. The labeled suspension was then applied to an LS column (Miltenyi Biotec, 130-042-401, Germany) placed in a MACS separator (Miltenyi Biotec, 130-090-976, Germany). After washing, the magnetically retained $CD11b^+$microglia were immediately eluted by firmly pressing the plunger into the column. For purity assessment, the sorted cells were stained with anti-CD11b-APC antibody (BioLegend, 101212, USA) for 20 min at 4°C, washed with PBS, and analyzed by flow cytometry.

3.9 Mitochondrial membrane potential (MMP) Assay

Purified mitochondria were extracted from magnetically sorted microglia using a Tissue Mitochondria Isolation Kit (Beyotime, C3606, China) according to the manufacturer's protocol. MMP was assessed using a JC-1 assay kit (Beyotime, C2006, China). Purified mitochondria were incubated with freshly prepared JC-1 staining working solution and incubated at 37°C for 30 min. Fluorescence intensities were measured using a multimode microplate reader (Spark, Tecan, Switzerland) with the following settings: JC-1 aggregates (red): Ex/Em=525/590nm and JC-1 monomers (green): Ex/Em=490/530 nm. The MMP levels were quantified as the ratio of red/green fluorescence intensity.

3.10 Isolation and Quantification of Cytosolic mtDNA by qPCR

Experimental procedures were carried out as previously described[20]. Briefly, the spinal cord tissue was homogenized in ice-cold buffer and subjected to differential centrifugation: first at 600g for 5 min at 4°C to pellet nuclei and intact cells, the lysate was centrifuged at 11,000g for 10 min at 4°C to remove mitochondria, and the resulting cytosolic supernatant was further clarified by centrifugation at 12,000g for 10 min at 4°C. Cytosolic DNA was then extracted from the final supernatant using a FastPure Blood/Cell/Tissue/Bacteria DNA Isolation Mini Kit (Vazyme, D102, China). QPCR was performed using SYBR qPCR Master Mix (Q311-02, Vazyme, China) in a 10 μl reaction volume with primers targeting mtDNA-encoded genes (Table 2). The thermocycling conditions were as follows: (1) Initial denaturation: 95°C for 30s; (2)

Amplification (40 cycles): 95°C for 10s(denaturation) and 60°C for 30s (annealing or extension); (3) Melting curve analysis:95°C for 15s, 60°C for 1 min and ramp to 95°C for 15s. Relative mtDNA levels were quantified using the $2^{-\Delta\Delta Ct}$ method and normalized to β-actin.

Table 2

Primers used for quantitative PCR assay.

Gene name	Forward/Reverse	Primer sequences (5'-3')
Dloop1	Forward	AATCTACCATCCTCCGTGAAACC
	Reverse	TCAGTTTAGCTACCCCCAAGTTTAA
Dloop2	Forward	CCCTTCCCCATTTGGTCT
	Reverse	TGGTTTCACGGAGGATGG
Dloop3	Forward	TCCTCCGTGAAACCAACAA
	Reverse	AGCGAGAAGAGGGGCATT
β-actin	Forward	GTGACGTTGACATCCGTAAAGA
	Reverse	GCCGGACTCATCGTACTCC

3.11 Mitochondrial Structures Observation by Transmission electron microscopy (TEM)

The deeply anesthetized mice were intracardially perfused with PBS followed by 2.5% glutaraldehyde fixative. Appropriately sized spinal cord tissue segments were immersed in 2.5% glutaraldehyde fixative overnight at 4°C. Following three washes with PBS, the tissues were fixed in 1% osmium tetroxide solution for 2h at RT. After dehydrated with ethanol, cleared in a transition solvent and embedded in resin, they were cut into 50nm-thick ultrathin sections and double-stained with 3% uranyl acetate and lead citrate. Mitochondrial structures were observed using a transmission electron microscope (Hitachi HT7700, Japan).

3.12 Detection of mitochondrial ROS

As described above, single-cell suspensions were extracted from spinal cord tissue and then washed with PBS. Cells were incubated with anti-CD11b-APC antibody (BioLegend, 101212, USA) for microglia identification and MitoSOX™ Red

Mitochondrial Superoxide Indicator (Invitrogen, M36007, USA) for 30 min at 37°C in the dark. After washing with PBS, fluorescence intensities were measured was measured by flow cytometry (BD Accuri, USA), Finally, mitochondrial ROS levels within the microglial population were analyzed using FlowJo software.

3.13 ATP Assay

ATP concentration in magnetically sorted microglia from isolated from fresh mouse spinal cord tissue were measured by ATP Assay Kit (Beyotime, S0026, China). Briefly, the collected cells were lysedin the provided buffer and homogenized using a Dounce homogenizer (Kimble, USA). The lysate was centrifuged at 12,000g for 10 min at 4°C, and 20μl of the supernatant was mixed with 100μl of ATP detection working solution in a 96-well black plate. Luminescence was immediately measured using a multimode microplate reader (Spark, Tecan, Switzerland). ATP content was calculated from a standard curve and normalized to total protein concentration.

3.14 Statistical Analysis

All experimental data are expressed as mean±standard error of the mean (SEM). Behavioral assessments over time were analyzed using two-way repeated-measures analysis of variance (ANOVA) followed by appropriate post hoc tests (Bonferroni test). Comparisons between two groups were performed using One-way analysis of variance (ANOVA). Statistical significance was defined as $p < 0.05$. All analyses were conducted using SPSS 22.0 and GraphPad Prism 9.0.

4.Results

4.1 Perioperative Sleep Deprivation Prolongs Postsurgical Pain Recovery and Enhances Spinal Microglial Activation

To evaluate the impact of sleep deprivation (SD) pretreatment on postoperative pain recovery, mice underwent 48 h of continuous SD prior to unilateral plantar incision surgery on the right hind paw (Fig 1). Behavioral testing showed no significant differences in baseline paw withdrawal thresholds (PWTs) among groups. Compared

with the control group, SD significantly reduced the mechanical PWT values, with the effect persisting for 5 days after sleep deprivation. (Con group vs. SD group). After surgery, control mice that underwent incision (Con+I) reached PMT nadir on postoperative day 1 and gradually recovered to control levels by day 9 (Con group vs. Con+I group) (Fig 2A). In contrast, sleep-deprived mice that underwent incision (SD+I) exhibited prolonged mechanical hypersensitivity, with PWTs remaining significantly lower than those in the Con+I group on postoperative days 7 and 9 (Con+I group vs. SD+I group), and persisting below baseline until day 14 before returning to control levels (Con group vs. SD+I group) (Fig 2A). These findings indicate that acute short-term SD pretreatment not only induces mechanical hypersensitivity on its own, but also synergizes with surgical trauma, significantly prolonged postsurgical pain recovery.

Next, L3-L5 spinal cord segments were harvested from Con+I group and SD+I group for immunofluorescence and western blot analysis on postoperative day 7 (Fig 1). The SD+I group exhibited higher Iba1 immunofluorescence intensity compared to Con+I group, indicating enhanced microglial activation in the spinal dorsal horn following SD (Fig. 2B-C). Western blot results demonstrated that the levels of the pro-inflammatory cytokines IL-1β, IL-6, and TNF-α were significantly upregulated in the SD+I group (Fig. 2D-G). Together, these findings suggest that SD pretreatment exacerbates and prolongs postsurgical pain, potentially through enhanced spinal microglial activation

and increased neuroinflammation.

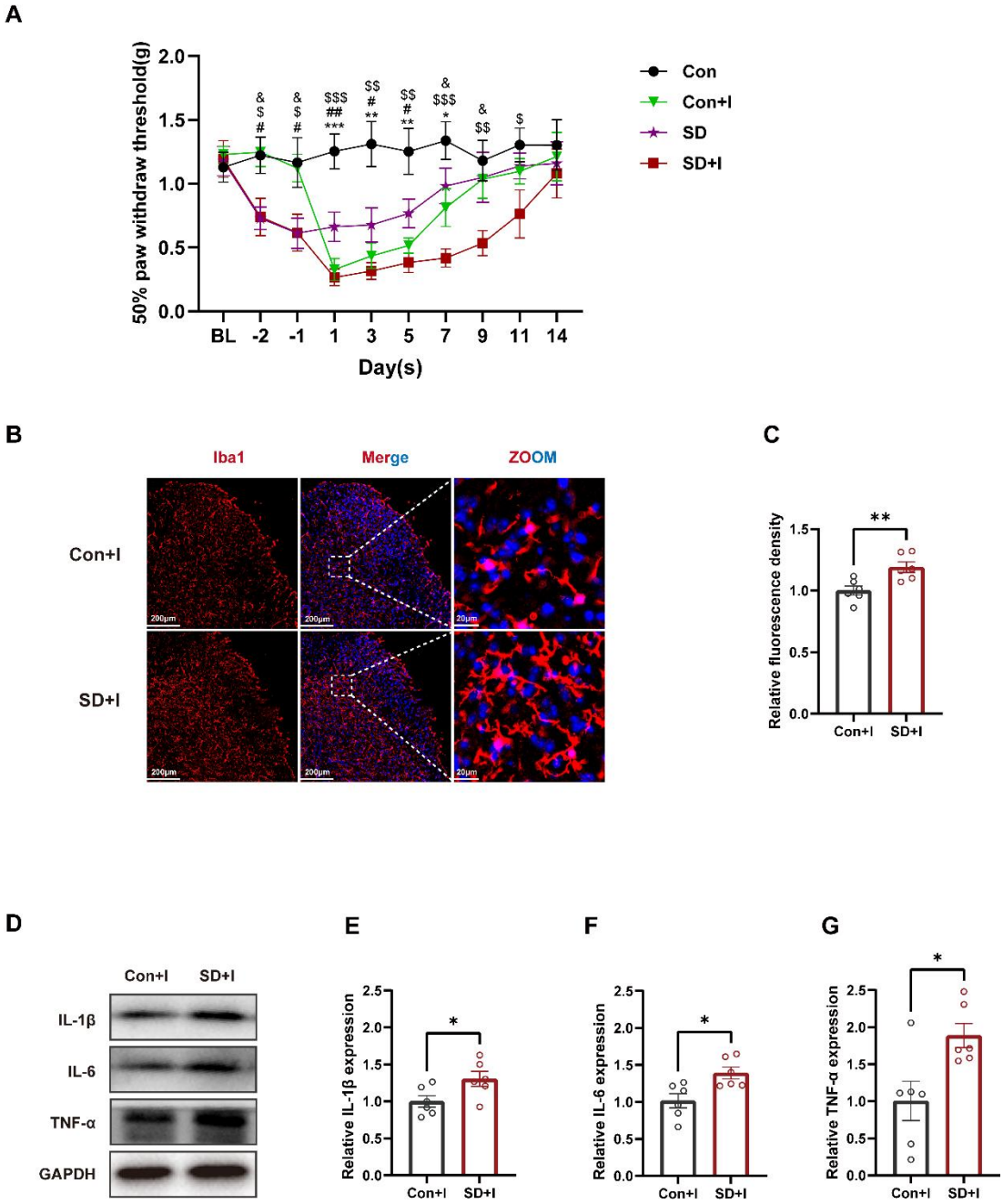


Fig 2. Pretreatment of 48h sleep deprivation promotes the transition to chronic post-surgical pain and spinal microglial activation. (A) Mechanical allodynia was evaluated using the 50% paw withdrawal threshold at baseline, during SD (Day -2 and -1) on the days post-incision (Day 1, 3, 5, 7, 9, 11 and 14). (Two-way ANOVA analysis. Con vs. Con+I: $^{*}p<0.05$, $^{**}p<0.01$, $^{***}p<0.001$; Con vs. SD: $^{\#}p<0.05$, $^{\#\#}p<0.01$; Con vs. SD+I: $^{\$}p<0.05$, $^{\$\$}p<0.01$, $^{\$\$\$}p<0.001$; Con+I vs. SD+I: $^{\&}p<0.05$, n=6 in each group). (B-C) Representative images and quantification fluorescence intensity of Iba1 immunofluorescence in the spinal dorsal horn on postoperative day 7. (Scale bars: 100μm, Con+I vs. SD+I: $^{**}p<0.01$, n=6 in each group). (D-G) Representative western blot images and quantitative analysis of pro-inflammatory cytokines IL-1β, IL-6 and TNF-α in spinal cord tissue collected on

postoperative day 7. (Con+I vs. SD+I: $^{*}p<0.05$ normalized to GAPDH, n=6 in each group).

4.2 Sleep Deprivation Promotes Mitochondrial Dysfunction and Cytosolic mtDNA Leakage in Spinal Microglia

Mitochondria serve as key organelles regulating microglial functional states, typically exhibit dysfunction prior to microglial activation and subsequent neuroinflammation[21, 22]. We therefore investigated whether this phenomenon occurred in SD+I mice to assess the impact of sleep deprivation on mitochondrial morphology and functional integrity in spinal microglia. Compared with Con+I group, spinal tissue from SD+I mice exhibited severe mitochondrial lesions, characterized by swelling, fragmentation, broken or absent cristae and compromised membrane integrity (Fig 3A).

Consistent with this morphological damage, SD+I mice exhibited significant elevated MitoROS levels in spinal microglia (Fig 3B-C). Further, we isolated spinal microglia via magnetic bead-based sorting and subjected them to ATP assay and JC-1 staining. The results showed a decrease in ATP production and the ratio of JC-1 aggregates to monomers, indicating impaired mitochondrial membrane potential and compromised energy production in the spinal microglia of SD+I mice compared with the Con+I group (Fig 3D-E). Collectively, these data suggest that sleep deprivation also disrupts the function of mitochondria in spinal microglia.

Given that mitochondrial damage frequently leads to mtDNA release into the cytosol[23, 24], we extracted cytosolic fractions from spinal cord tissues and quantified mtDNA levels using qPCR to quantify the amount of mtDNA released to the cytosol (Fig 3F). The results showed that the levels of mitochondrial D-loop region including Dloop1, Dloop2 and Dloop3 in the cytoplasm of the SD+I group were significantly higher than those of the Con+I group (Fig 3G).

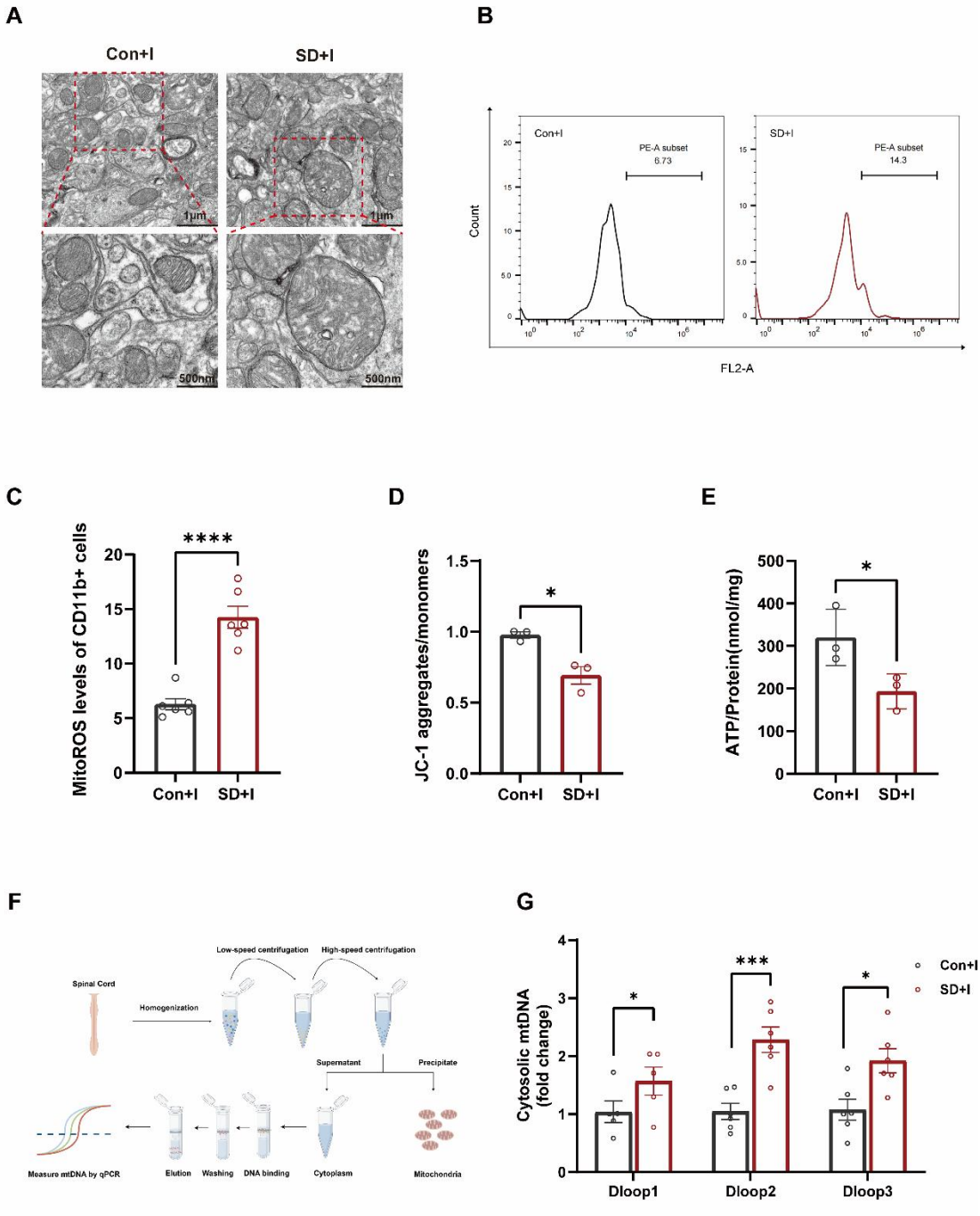


Fig 3. Spinal microglia in SD+I mice exhibit mitochondrial dysfunction accompanied by aberrant cytosolic mtDNA accumulation. (A) Representative transmission electron microscopy images showing mitochondrial ultrastructure in spinal dorsal horn on postoperative day 7. (Scale bars: 1μm, 500nm). (B-C) The MitoROS level of spinal microglia in mice was determined by flow cytometry (n=6 in each group). (D) Quantification of mitochondrial membrane potential in isolated spinal microglia, assessed by JC-1 staining following magnetic bead-based microglial purification. (n=3 in each group). (E) Measurement of ATP levels in isolated spinal microglia. (n=3 in each group). (F) Experimental schematic illustrates the workflow for quantifying cytosolic mtDNA by qPCR in

cytosolic fractions isolated from spinal cord tissue. (G) Quantification of cytosolic mtDNA, including D-loop1, D-loop2, and D-loop3, in cytosolic fractions of spinal cord tissue (n=3 in each group). All data were expressed as mean±SEM, Con+I vs. SD+I: $^{*}p<0.05$, $^{***}p<0.001$, $^{****}p<0.0001$.

4.3 MitoROS Accumulation Drives Mitochondrial Dysfunction and mtDNA Leakage

MitoROS serves as the most important marker of mitochondrial damage, and its excessive accumulation can trigger oxidative stress, mitochondrial dysfunction, inflammatory responses, and ultimately cell death[22]. To investigate whether MitoROS acts as the initiating factor for mitochondrial dysfunction and subsequent mtDNA leakage in microglia, the mitochondrial-targeted antioxidant Mito-Tempo was administered to scavenge MitoROS in the mouse model of continuous 48-hour sleep deprivation combined with plantar incision surgery. Mice received daily intraperitoneal injections of Mito-Tempo beginning one day prior to sleep deprivation and continuing until postoperative day 7, after which spinal cord tissues were collected for analysis, with a parallel control group (SD+I+Veh) receiving equivalent volumes of saline injections (Fig. 1).

Administration of the mitochondria-targeted antioxidant Mito-Tempo effectively prevented the accumulation of MitoROS, in spinal microglia compared with the SD+I+Veh group (Fig. 4A-B). Transmission electron microscopy revealed pronounced mitochondrial swelling, disrupted outer membranes, and fragmented or absent cristae in the SD+I+Veh group, whereas mitochondria in the SD+I+Mito-Tempo group exhibited intact membranes and well-organized cristae, indicating structural restoration of mitochondria following Mito-Tempo treatment (Fig. 4C). Moreover, JC-1 staining and ATP assays revealed increased mitochondrial membrane potential and elevated ATP levels in the SD+I+Mito-Tempo group, suggesting improved mitochondrial function after MitoROS scavenging (Fig. 4D-E). Furthermore, Mito-Tempo-mediated clearance of MitoROS significantly prevented mtDNA escape from mitochondria to the cytoplasm in the spinal cord, as evidenced by reduced cytoplasmic accumulation of D-loop DNA fragments in the SD+I+Mito-Tempo group (Fig. 4F).

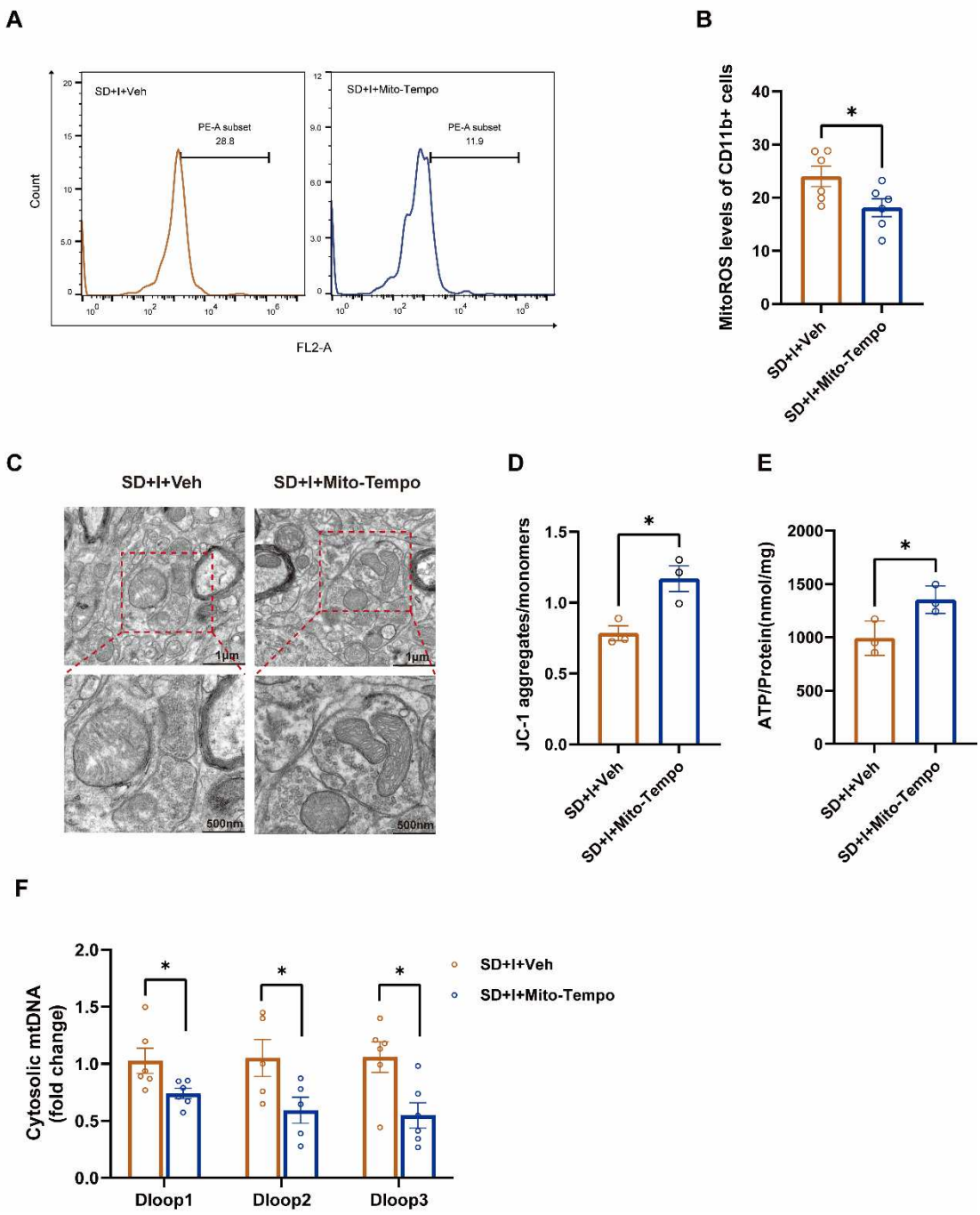


Fig 4. Scavenging MitoROS restores mitochondrial integrity and reduces cytosolic mtDNA leakage in spinal microglia. (A-B) Flow cytometry analysis confirming the efficacy of Mito-Tempo treatment in reducing MitoROS levels in spinal microglia. (n=6 in each group). (C) Representative transmission electron microscopy images of mitochondrial ultrastructure in the spinal dorsal horn on postoperative day 7 (Scale bars: 1μm, 500nm). (D) Quantification of mitochondrial membrane potential in isolated spinal microglia (n=3 in each group). (E) Measurement of ATP levels in isolated spinal microglia. (n=3 in each group). (F) Quantification of cytosolic mtDNA D-loops in cytosolic fractions of spinal cord tissue (n=3 in each group). All data were expressed as mean ± SEM, SD+I+Veh vs. SD+I+Mito-Tempo: $^{*}p<0.05$.

4.4 Scavenging MitoROS Alleviates Sleep Deprivation-Induced Spinal Neuroinflammation and Hyperalgesia

Behavioral assessments revealed that PWT values were significantly higher in the SD+I+Mito-Tempo group compared to the SD+I+Veh group on postoperative days 7, 9, and 11, indicating that Mito-Tempo treatment effectively alleviated sleep deprivation-induced postoperative hyperalgesia (Fig. 5A). Consistent with these behavioral improvements, immunofluorescence analysis showed that Mito-Tempo administration markedly suppressed microglial activation in the spinal cord (Fig. 8B-C), as evidenced by a substantial reduction in the relative fluorescence intensity of Iba1 (Fig. 5B-C). Furthermore, Western blot analysis showed that the spinal expression of pro-inflammatory cytokines, including IL-1β, IL-6, and TNF-α, was significantly downregulated following Mito-Tempo treatment (Fig. 5D-G).

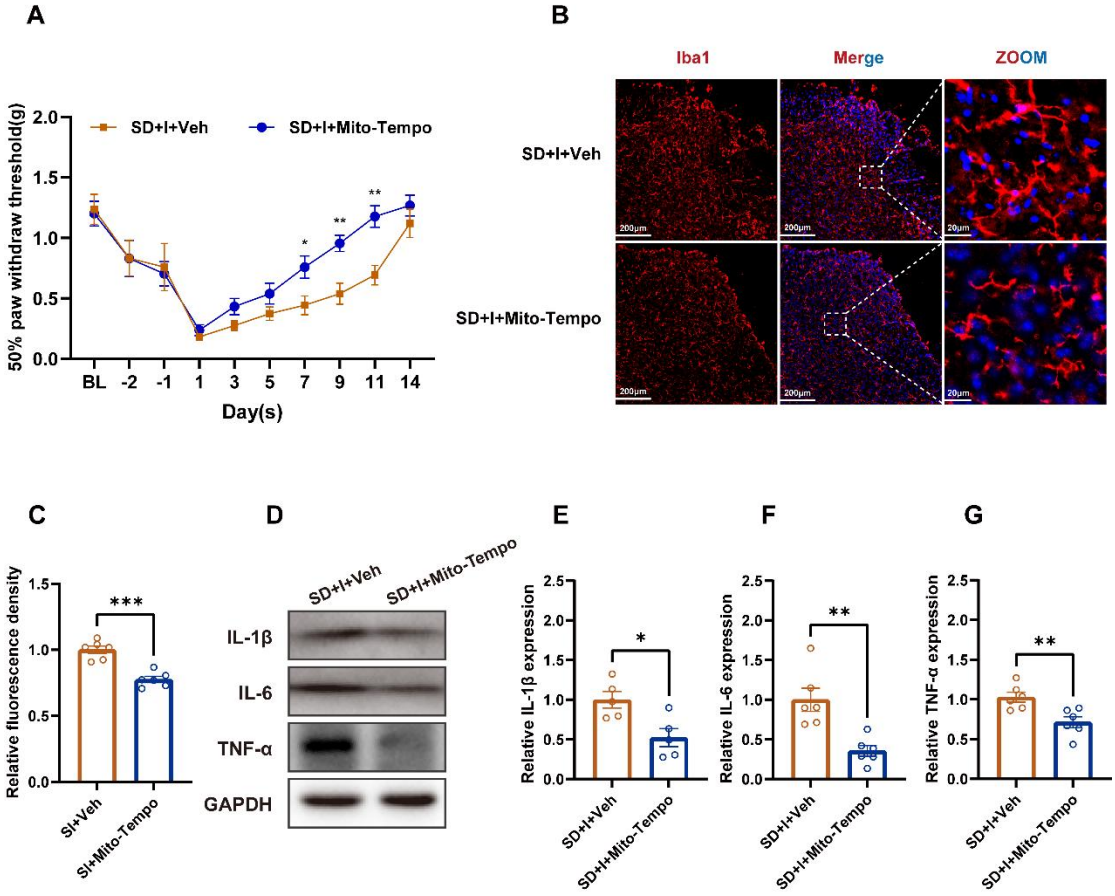


Fig 5. Mito-Tempo also mitigates microglial activation and alleviates sleep deprivation-induced mechanical allodynia. (A) Time course of 50% paw withdrawal threshold showing the analgesic effect of Mito-Tempo treatment shortened the duration of postoperative hyperalgesia

induced by sleep deprivation (n=6 in each group). (B-C) Iba1 Immunofluorescence staining of spinal cord sections illustrating the effect of Mito-Tempo on microglial activation state (Scale bar: 200μm, n=6 in each group). (D-G) Western blot analysis of IL-1β, IL-6, and TNF-α in spinal cord tissue showing that Mito-Tempo treatment downregulated the expression of these pro-inflammatory cytokines (normalized to GAPDH, n=6 in each group). All data were expressed as mean±SEM, SD+I+Veh vs. SD+I+ Mito-Tempo: $^{*}p<0.05$, $^{**}p<0.01$, $^{***}p<0.001$.

4.5 Sleep Deprivation activates mtDNA-cGAS-STING pathway in Spinal Microglia

The cGAS-STING pathway, a component of the innate immune system closely associated with neuroinflammatory disorders, has been identified as a critical cytoplasmic DNA sensor and downstream effector molecules[25]. Following our findings of cytosolic mtDNA leakage, we next assessed the effects of sleep deprivation on cGAS-STING signaling pathway activation. To evaluate pathway activation, spinal cord tissues were collected on postoperative day 7, and the expression levels of key components of the cGAS-STING pathway were assessed by western blot and immunofluorescence staining. Western blot analysis revealed that, compared with the Con+I group, mice in the SD+I group exhibited significantly increased protein levels of cGAS, p-STING, p-TBK1 and p-IRF3. In contrast, the total protein levels of STING, TBK1, and IRF3 showed no significant difference between the two groups, indicating that sleep deprivation primarily induced pathway activation through enhanced phosphorylation rather than altered total protein expression (Fig. 6A-H). Meanwhile, immunofluorescence double staining revealed a high degree of colocalization between STING and the microglial marker Iba1 in the spinal cord of SD+I group mice, indicating that SD-induced the cGAS-STING pathway activation occurred in microglia (Fig. 7I-J). Together, these data indicate that sleep deprivation induces activation of the microglial cGAS-STING signaling cascade in the spinal cord, consistent with cytosolic mtDNA acting as an upstream trigger for this innate immune response.

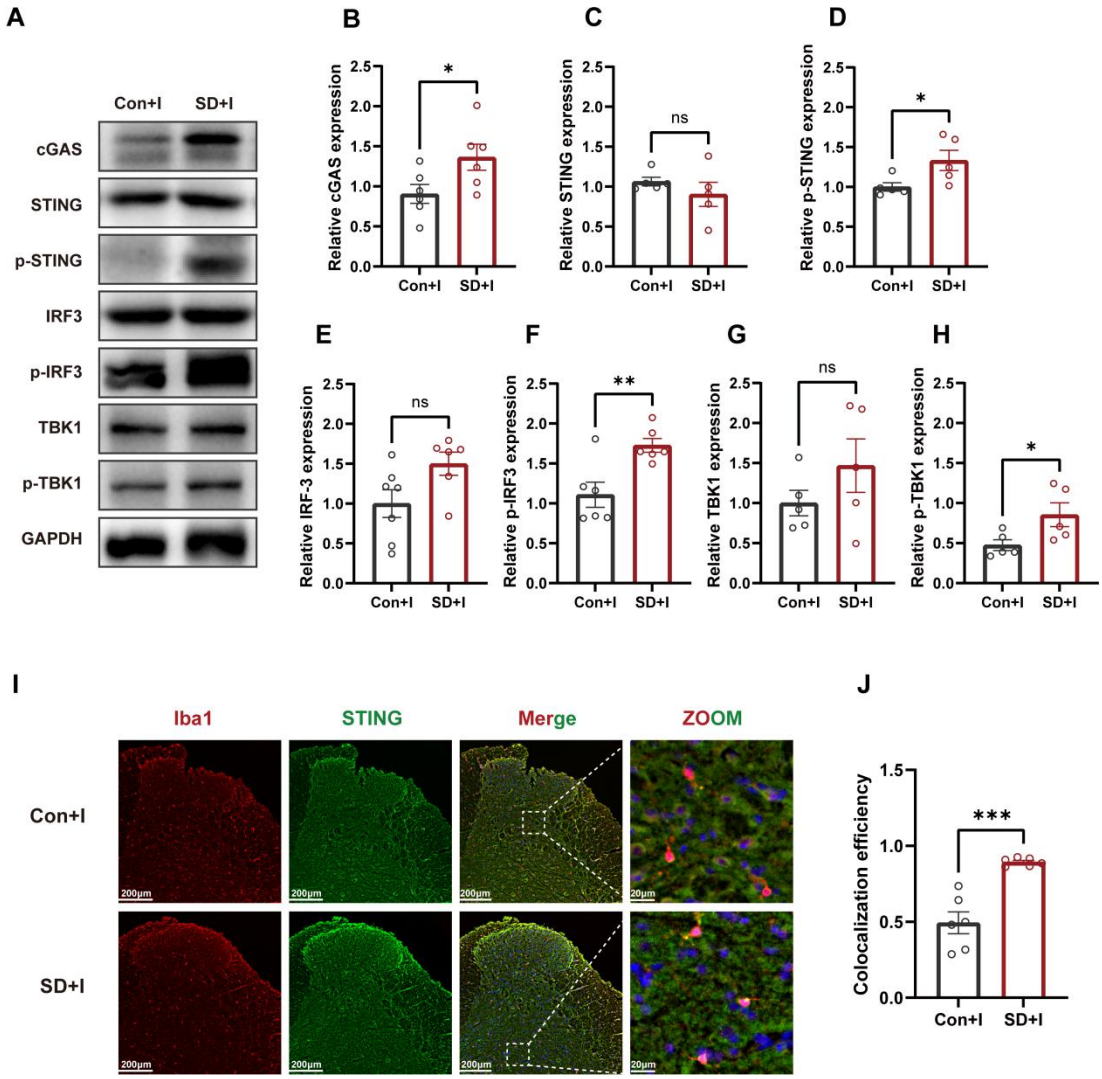


Fig 6. The STING signaling pathway is activated in spinal microglia of SD+I mice. (A-H) Representative western blot images and quantitative analysis of key components of the cGAS-STING pathway, including cGAS, STING, p-STING, IRF3, p-IRF3, TBK1, p-TBK1, in spinal cord tissue collected on postoperative day 7. (normalized to GAPDH, n=6 in each group). (I-J) Double immunofluorescence staining and colocalization analysis of STING and Iba1 in the spinal dorsal horn on postoperative day 7 (Scale bar: 200μm, n=6 in each group). All data were expressed as mean±SEM, Con+I vs. SD+I: $^{*}p<0.05$, $^{**}p<0.01$, $^{***}p<0.001$.

4.6 The STING Inhibitor C-176 Attenuates Sleep Deprivation-Induced Spinal Neuroinflammation and Hyperalgesia

To further explore whether the cGAS-STING signaling pathway in the spinal dorsal horn is involved in the process of sleep deprivation-induced spinal neuroinflammation and hyperalgesia, we next administered the selective STING inhibitor C-176 intraperitoneally beginning one day before sleep deprivation, followed by daily

injections until postoperative day 14. During this period, spinal cord tissues were collected on postoperative day 7 for Western blot and immunofluorescence analyses to examine the corresponding molecular changes, while behavioral assessments were conducted to evaluate pain sensitivity by measuring alterations in mechanical withdrawal thresholds (Fig 1).

Western blot analysis demonstrated that treatment with C-176 effectively attenuated the expression of the key pathway proteins cGAS, STING, and p-STING in the spinal cord, confirming the effective inhibition of STING signaling by C-176 (Fig 7A-D). Behavioral testing revealed no significant differences in PWT values between the SD+I+C-176 and SD+I+Veh groups during the sleep deprivation period. However, on postoperative days 5, 7, and 9, PWT values were markedly increased in the C-176-treated group, indicating a shortened duration and reduced severity of sleep deprivation-induced postoperative mechanical hyperalgesia (Fig. 7E). Immunofluorescence staining revealed a significant reduction in Iba1-positive microglia in the spinal dorsal horn of SD+I+C-176 mice compared with the SD+I+Veh group, suggesting decreased microglial activation on postoperative day 7 (Fig. 7F-G).Consistently, the expression of the core pro-inflammatory cytokines IL-1β, IL-6, and TNF-α in the spinal cord were effectively downregulated following C-176 treatment, suggesting effective inhibition of spinal neuroinflammation (Fig 7H-K). Collectively, the aforementioned results showed that pharmacological inhibition of STING signaling by C-176 effectively

alleviate sleep deprivation-induced microglial activation and spinal neuroinflammation, ultimately promoting postoperative pain recovery.

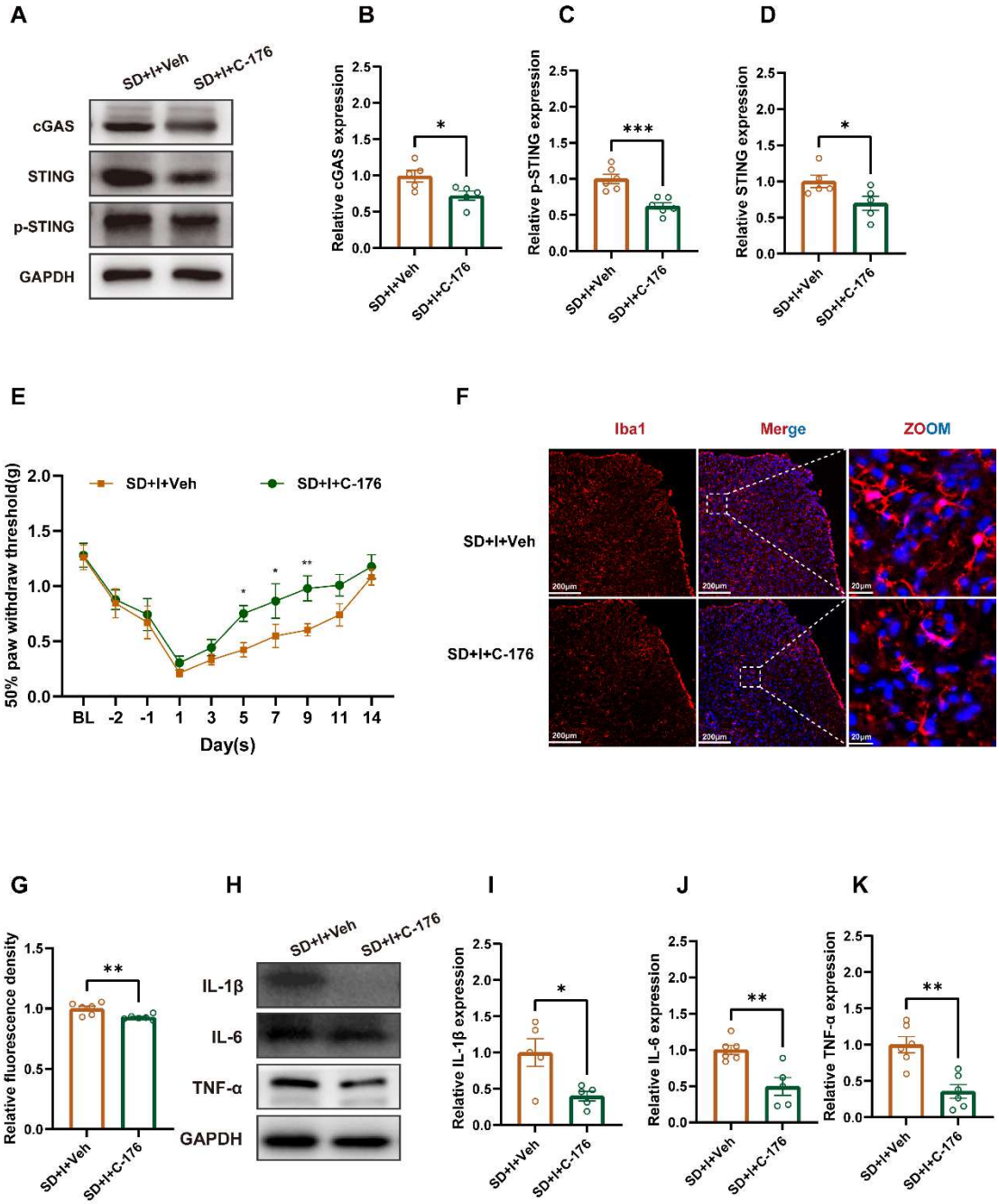


Fig 7. C-176 mitigates microglial activation and alleviates sleep deprivation-induced mechanical allodynia. (A-D) Western blot analysis of spinal cord tissue showing protein levels of cGAS, STING, and p-STING, confirming the inhibitory effect of the STING-specific antagonist C-176. (E) Time course of 50% paw withdrawal threshold showing the analgesic effect of C-176 treatment shortened the duration of postoperative hyperalgesia induced by sleep deprivation (n=6 in each group). (F-G) Iba1 Immunofluorescence staining of spinal cord sections illustrating the effect of C-176 on microglial activation state (Scale bar: 200μm, n=6 in each group). (H-K) Western blot analysis of IL-1β, IL-6, and TNF-α in spinal cord tissue showing that C-176 treatment

downregulated the expression of these pro-inflammatory cytokines (normalized to GAPDH, n=6 in each group). All data were expressed as mean±SEM, SD+I+Veh vs. SD+I+C-176: $^{*}p<0.05$, $^{**}p<0.01$, $^{***}p<0.001$.

4.7 Mito-Tempo Targets the mtDNA-cGAS-STING Pathway to Suppress Neuroinflammation and Pain

Next, we examined whether MitoROS acts upstream to activate the cGAS-STING pathway and modulates sleep deprivation-induced postoperative hyperalgesia. Administration of the Mito-Tempo resulted in a marked attenuation of cGAS protein expression and a significant reduction in the phosphorylation levels of STING, TBK1, and IRF3. In contrast, the total protein levels of these signaling molecules remained unchanged between groups (Fig. 7A-H). Immunofluorescence double staining further demonstrated decreased colocalization between STING and Iba1 in the SD+I+Mito-Tempo group, indicating that Mito-Tempo reversed the sleep deprivation-induced activation of STING in spinal microglia (Fig. 7I-J). These findings demonstrate that MitoROS accumulation serves as a critical upstream trigger for the activation of the microglial cGAS-STING signaling cascade. Consequently, these findings demonstrate that MitoROS accumulation is essential for microglial cGAS-STING signaling, and pharmacological scavenging of MitoROS suppresses this signaling cascade, alleviating neuroinflammation and promoting recovery from sleep deprivation-induced postoperative hyperalgesia.

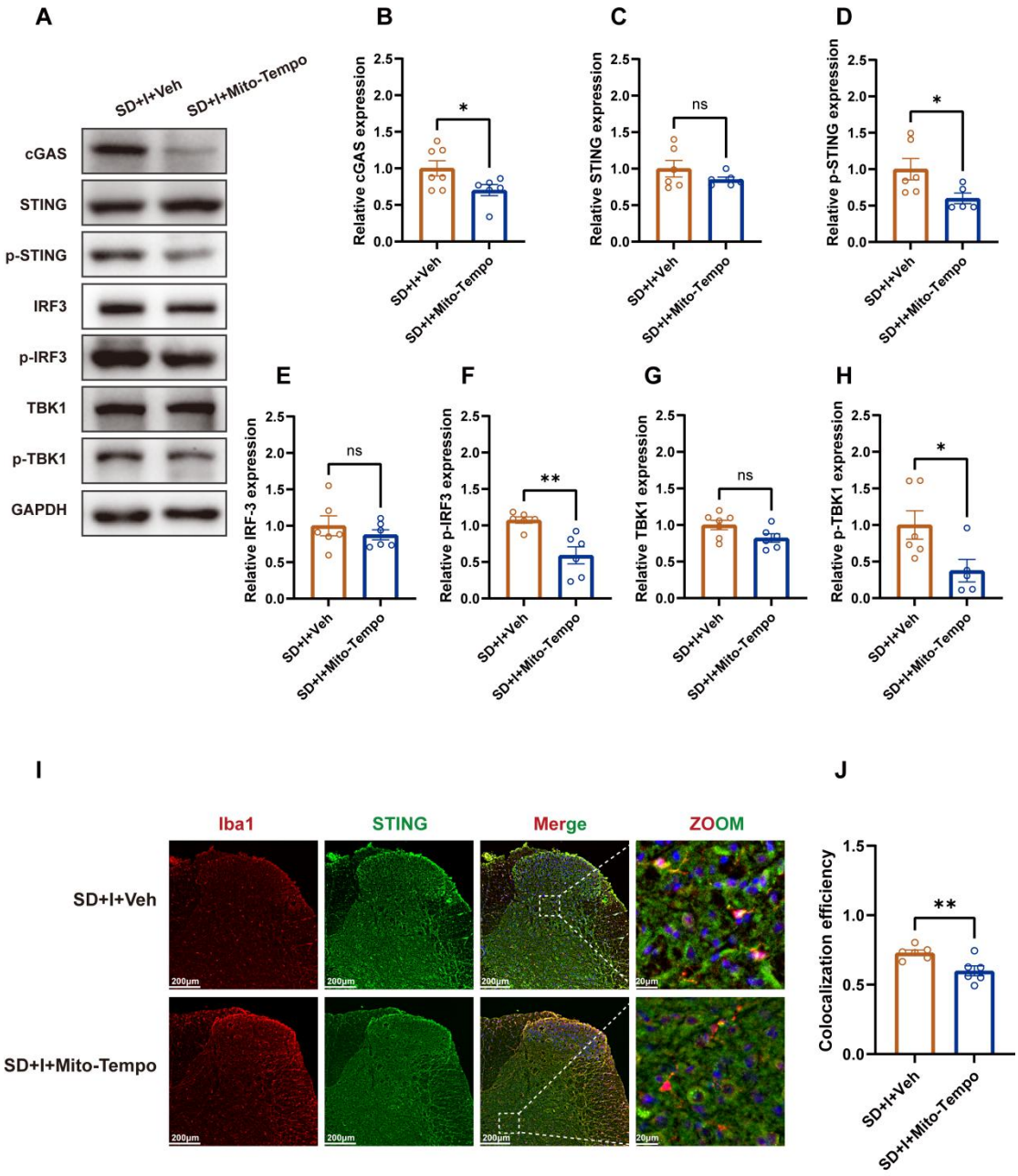


Fig 8. Mito-Tempo suppresses sleep deprivation-induced activation of the cGAS-STING pathway in the spinal cord. (A-H) Representative western blot images and quantitative analysis of key components of the cGAS-STING pathway in spinal cord tissue collected on postoperative day 7. (normalized to GAPDH, n=6 in each group). (I-J) Double immunofluorescence staining and colocalization analysis of STING and Iba1 in the spinal dorsal horn on postoperative day 7. (Scale bar: 200μm, n=6 in each group). All data were expressed as mean±SEM, SD+I+Veh vs. SD+I+Mito-Tempo: $^{*}p<0.05$, $^{**}p<0.01$.

5.Discussion

This study showed that: (1) Preoperative sleep deprivation significantly prolonged the duration of postoperative mechanical hyperalgesia; (2) Sleep deprivation induced excessive accumulation of MitoROS in spinal microglia, leading to mitochondrial structural and functional impairment as well as cytosolic leakage of mtDNA; (3) The released mtDNA subsequently activated the cGAS-STING signaling pathway, driving microglial activation and the production of inflammatory cytokines, thereby mediating sleep deprivation-induced postoperative hyperalgesia; (4) Pharmacological interventions using the selective STING inhibitor C-176 or the mitochondria-targeted antioxidant Mito-Tempo effectively attenuated sleep deprivation-induced microglial activation, spinal neuroinflammation, and persistent postoperative hyperalgesia.

Current clinical evidence clearly establishes sleep deprivation as a significant risk factor for the development of chronic postsurgical pain[26, 27]. Complementing these clinical observations, experimental evidence increasingly indicates that sleep deprivation exacerbates pain sensitivity across various rodent pain models, including neuropathic pain, formalin-induced inflammatory pain, and skin/muscle incision and retraction (SMIR) surgery[28-30]. Similar to what was previously reported[10], we utilized a plantar incision model to mimic acute surgical pain in humans in the present study, we observed that sleep deprivation alone is sufficient to induce a decline in mechanical pain thresholds in mice. And sleep deprivation not only intensifies the magnitude of postoperative hyperalgesia, but also significantly extends its duration, reinforcing the notion that sleep loss is a potent driver of pain chronification.

Activation of spinal microglia and the subsequent glia-neuron interactions are key steps of central sensitization and pain persistence. In our study, perioperative sleep deprivation induces spinal microglial activation and the release of pro-inflammatory cytokines such as IL-1β and TNF-α. According to previous studies, these microglia-derived cytokines activate Src family kinases (SFKs) in adjacent neurons, leading to phosphorylation of NMDA receptor subunits NR1 and NR2B[31]. And they promote the trafficking of AMPA receptor GluA1 subunits to the postsynaptic membrane via PI3K-

and PKA-dependent pathways, thereby enhancing glutamate release and excitatory synaptic transmission[32, 33]. Furthermore, these cytokines modulate the frequency, amplitude, and kinetics of spontaneous inhibitory postsynaptic currents (sIPSCs) and directly inhibit GABAergic and glycinergic receptor activity, thereby weakening inhibitory synaptic transmission[34, 35]. Collectively, perioperative sleep deprivation may act as a stressor that triggers spinal inflammatory responses via microglial activation, disrupts the excitatory–inhibitory balance of neurons, and ultimately contributes to the development of central sensitization.

Our findings demonstrate that sleep deprivation combined with incisional surgery exacerbates structural and functional impairments in microglial mitochondria. As the central organelles of cellular energy metabolism, mitochondrial dysfunction triggers profound metabolic reprogramming in microglia. Impaired oxidative phosphorylation (OXPHOS) promotes a compensatory shift toward glycolysis, generating metabolites such as lactate that activate pro-inflammatory pathways, including HIF-1α, thereby inducing microglial phenotypic transitions and central neuroinflammation[36, 37]. Moreover, impaired mitochondrial fatty acid oxidation leads to abnormal lipid droplet accumulation, which disrupt microglial synaptic pruning through downregulating key enzymes, thereby contributing to the amplification of pain signaling[38]. A study revealed that promoting microglial mitophagy to remove damaged mitochondria effectively suppressed NLRP3 inflammasome activation and alleviated chronic neuropathic pain in mice[39]. Notably, mitochondrial dysfunction also participates in deeper glia-neuron material exchange. Vesicles derived from damaged mitochondria can carry mitochondrial components such as mtDNA or metabolic enzymes, thereby altering neuronal metabolic states[40]. The recent study further indicates that mitochondria can even be directly transferred into neurons[41]. Such interactions may facilitate stress signal propagation or the transfer of dysfunctional mitochondria under pathological conditions. Therefore, future studies are needed to elucidate how glia-neuron metabolic coupling sustains the chronicization of postoperative pain induced by

sleep deprivation.

In the progression of mitochondrial damage, the abnormal accumulation of mtROS serves as a central driver[42, 43]. Peruzzotti-Jametti et al. reported that upregulation of mitochondrial complex I drives reverse electron transport, resulting in the persistent production of MitoROS, which maintains microglial activation and sustains CNS inflammation[44]. Consistently, our results showed that markedly elevated MitoROS levels in spinal microglia in the SD+I group, accompanied by increased cytosolic mtDNA. Excess MitoROS can directly damage mitochondrial membranes and respiratory chain components[45], and induce persistent opening of the mitochondrial permeability transition pore (mPTP) through redox-sensitive mechanisms[46]. This disruption of membrane integrity facilitates the release of mitochondrial damage-associated molecular patterns (DAMPs) into the cytosol[47]. Among them, mtDNA release is one of the most potent pro-inflammatory events[48]. Under physiological conditions, mtDNA is sequestered within the matrix and anchored by nucleoid structures, protected by the dual-layer membrane barrier. However, MitoROS-induced damage enables its escape into the cytoplasm via sustained mPTP opening or voltage-dependent anion channel 1 (VADC1) oligomerization [49, 50]. Our results showed that scavenging MitoROS restored mitochondrial structure, membrane potential, and ATP production, while preventing cytosolic mtDNA accumulation in mice subjected to the sleep deprivation-postoperative pain model. This reversal effect provides evidence that mtROS act as a critical upstream mediator of mitochondrial dysfunction and mtDNA release.

Emerging evidence indicates that cGAS not only functions as a major sensor of microbial DNA but also as a key detector of mislocalized cytosolic DNA under pathological conditions[51]. Upon sensing leaked mtDNA, cGAS catalyzes the synthesis of cGAMP, which activates STING and subsequently triggers TBK1 phosphorylation, IRF3 nuclear translocation, and the production of type I interferons and proinflammatory cytokines[52]. Previous studies have reported both pro- and anti-nociceptive roles of the cGAS-STING pathway depending on the specific cell types and

pain models[53]. For example, Donnelly et al. found that STING deletion increased the excitability of nociceptors, suggesting an antinociceptive role[54], whereas other studies reported that STING activation promoted microglial M1 polarization and mechanical allodynia in models such as spared nerve injury and bone cancer pain[55-57]. Our results support the pro-nociceptive role of this pathway, as evidenced by increased STING expression and its colocalization with the microglial marker Iba1. Pharmacological inhibition of STING with C-176 reduced proinflammatory cytokine levels and alleviated mechanical hypersensitivity, indicating that microglial cGAS-STING activation contributes to chronic postoperative pain. Furthermore, the mitochondria-targeted antioxidant Mito-Tempo suppressed STING signaling, accompanied by reduced cytokine production and pain sensitivity. These results provide direct evidence that excessive MitoROS act as an upstream driver of mtDNA release, thereby triggering aberrant activation of the cGAS-STING signaling cascade.

This study had some limitations. First, mitochondrial morphology, function, and MitoROS levels were evaluated only on postoperative day 7, limiting temporal insight into the dynamic changes during pain initiation and resolution. Second, although our results implicate MitoROS in mtDNA leakage, the precise molecular mechanism underlying this process remains to be defined. Possible mediators include oxidative damage to mtDNA, disruption of mitochondrial outer membrane integrity, or regulated pore formation via VDAC1 oligomerization or BAK/BAX pore[58, 59]. Finally, systemic intraperitoneal drug administration may have introduced off-target effects in non-neural tissues such as the liver or kidneys. Future studies could utilize intrathecal delivery or nanocarrier-based targeted delivery to enhance spinal specificity and therapeutic efficacy while minimizing systemic side effects.

6. Conclusions

In summary, our findings identify mitochondrial oxidative stress and the downstream mtDNA-cGAS-STING signaling pathway in spinal microglia as central mediators of sleep deprivation-induced postoperative hyperalgesia, providing mechanistic insight

and novel therapeutic strategies for the prevention of chronic postsurgical pain in patients with perioperative sleep disturbances.

7. References

[1] ANTILA H, LILIUS T O, PALADA V, et al. Effects of commonly used analgesics on sleep architecture-A topical review [J]. Pain, 2024.

[2] TANG S, JIN Y, HOU Y, et al. Predictors of Chronic Pain in Elderly Patients Undergoing Total Knee and Hip Arthroplasty: A Prospective Observational Study [J]. J Arthroplasty, 2023, 38(9): 1693-9.

[3] CHEN D, YANG H, YANG L, et al. Preoperative psychological symptoms and chronic postsurgical pain: analysis of the prospective China Surgery and Anaesthesia Cohort study [J]. Br J Anaesth, 2023.

[4] PU W, ZHOU L, LIU R, et al. Microglia-derived neuroinflammatory pathways in neuropathic pain [J]. Korean J Pain, 2025.

[5] LIU Y C, CHIU B Y, TU K Y, et al. Intermittent Hypoxia Triggers Glial Cell Activation, GluN2B Receptor Upregulation and Hyperalgesia in a Mouse Model of Sleep Apnea [J]. Eur J Pain, 2025, 29(6): e70039.

[6] YANG H, ZHANG Y, DUAN Q, et al. Dehydrocorydaline alleviates sleep deprivation-induced persistent postoperative pain in adolescent mice through inhibiting microglial P2Y12 receptor expression in the spinal cord [J]. Mol Pain, 2023, 19: 17448069231216234.

[7] WILLEMEN H, SANTOS RIBEIRO P S, BROEKS M, et al. Inflammation-induced mitochondrial and metabolic disturbances in sensory neurons control the switch from acute to chronic pain [J]. Cell Rep Med, 2023, 4(11): 101265.

[8] AWAD-IGBARIA Y, BEN-MENASHE A, SAKAS R, et al. Novel insight into TRPV1-induced mitochondrial dysfunction in neuropathic pain [J]. Brain, 2025.

[9] WU L, LIN T, ZHANG Z, et al. Ginsenoside Rg1 improves chronic neuropathic pain by inhibiting NLRP3 inflammasome activation and cell pyroptosis in microglia [J]. J Ethnopharmacol, 2025: 120346.

[10] HUANG Y, HAO J, YANG X, et al. Pretreatment of the ROS Inhibitor Phenyl-N-tert-butylnitrone Alleviates Sleep Deprivation-Induced Hyperalgesia by Suppressing Microglia Activation and NLRP3 Inflammasome Activity in the Spinal Dorsal Cord [J]. Neurochem Res, 2023, 48(1): 305-14.

[11] MARCHI S, GUILBAUD E, TAIT S W G, et al. Mitochondrial control of inflammation [J]. Nat Rev Immunol, 2023, 23(3): 159-73.

[12] WANG Z, WU H, CHANG X, et al. CKMT1 deficiency contributes to mitochondrial dysfunction and promotes intestinal epithelial cell apoptosis via reverse electron transfer-derived ROS in colitis [J]. Cell Death Dis, 2025, 16(1): 177.

[13] GIORDANO L, WARE S A, LAGRANHA C J, et al. Mitochondrial DNA signals driving immune responses: Why, How, Where? [J]. Cell Commun Signal, 2025, 23(1): 192.

[14] HE S, LI X, MITTRA N, et al. Microglial cGAS Deletion Preserves Intercellular Communication and Alleviates Amyloid-β-Induced Pathogenesis of Alzheimer's Disease [J]. Adv Sci (Weinh), 2025: e2410910.

[15] ZHANG W, LI G, LUO R, et al. Cytosolic escape of mitochondrial DNA triggers cGAS-STING-NLRP3 axis-dependent nucleus pulposus cell pyroptosis [J]. Exp Mol Med, 2022, 54(2): 129-42.

[16] BRENNAN T J, VANDERMEULEN E P, GEBHART G F. Characterization of a rat model of incisional pain [J]. Pain, 1996, 64(3): 493-502.

[17] HU J, JI W J, LIU G Y, et al. IDO1 modulates pain sensitivity and comorbid anxiety in chronic migraine through microglial activation and synaptic pruning [J]. J Neuroinflammation, 2025, 22(1): 42.

[18] SHENG H, HUANG Y, XIAO Y, et al. ATR inhibitor AZD6738 enhances the antitumor activity of radiotherapy and immune checkpoint inhibitors by potentiating the tumor immune microenvironment in hepatocellular carcinoma [J]. J Immunother Cancer, 2020, 8(1).

[19] ZHAN L, LI R, SUN Y, et al. Effect of mito-TEMPO, a mitochondria-targeted antioxidant, in rats with neuropathic pain [J]. Neuroreport, 2018, 29(15): 1275-81.

[20] CHEN Y, HU Y, HE X, et al. Activation of mitochondrial DNA-mediated cGAS-STING pathway contributes to chronic postsurgical pain by inducing type I interferons and A1 reactive astrocytes in the spinal cord [J]. Int Immunopharmacol, 2023, 127: 111348.

[21] PARHIZKAR S, GENT G, CHEN Y, et al. Sleep deprivation exacerbates microglial reactivity and Aβ deposition in a TREM2-dependent manner in mice [J]. Sci Transl Med, 2023, 15(693): eade6285.

[22] CHENG Y, GU W, WU X, et al. Allicin alleviates traumatic brain injury-induced neuroinflammation by enhancing PKC-δ-mediated mitophagy [J]. Phytomedicine, 2025, 139: 156500.

[23] HE B, YU H, LIU S, et al. Mitochondrial cristae architecture protects against mtDNA release and inflammation [J]. Cell Rep, 2022, 41(10): 111774.

[24] DU Q, NING N, ZHAO X, et al. Acylglycerol kinase inhibits macrophage anti-tumor activity via limiting mtDNA release and cGAS-STING-type I IFN response [J]. Theranostics, 2025, 15(4): 1304-19.

[25] ZHANG Z, ZHANG C. Regulation of cGAS-STING signalling and its diversity of cellular outcomes [J]. Nat Rev Immunol, 2025.

[26] VARALLO G, GIUSTI E M, MANNA C, et al. Sleep disturbances and sleep disorders as risk factors for chronic postsurgical pain: A systematic review and meta-analysis [J].

Sleep Med Rev, 2022, 63: 101630.

[27] WANG J P, LU S F, GUO L N, et al. Poor preoperative sleep quality is a risk factor for severe postoperative pain after breast cancer surgery: A prospective cohort study [J]. Medicine (Baltimore), 2019, 98(44): e17708.

[28] WEI S N, ZHANG H, LU Y, et al. Microglial voltage-dependent anion channel 1 signaling modulates sleep deprivation-induced transition to chronic postsurgical pain [J]. Sleep, 2023, 46(11).

[29] VANINI G. Sleep Deprivation and Recovery Sleep Prior to a Noxious Inflammatory Insult Influence Characteristics and Duration of Pain [J]. Sleep, 2016, 39(1): 133-42.

[30] HUANG C T, CHIANG R P, CHEN C L, et al. Sleep deprivation aggravates median nerve injury-induced neuropathic pain and enhances microglial activation by suppressing melatonin secretion [J]. Sleep, 2014, 37(9): 1513-23.

[31] CHEN G, ZHANG Y Q, QADRI Y J, et al. Microglia in Pain: Detrimental and Protective Roles in Pathogenesis and Resolution of Pain [J]. Neuron, 2018, 100(6): 1292-311.

[32] KLEIDONAS D, KIRSCH M, ANDRIEUX G, et al. Microglia modulate TNFα-mediated synaptic plasticity [J]. Glia, 2023, 71(9): 2117-36.

[33] WIGERBLAD G, HUIE J R, YIN H Z, et al. Inflammation-induced GluA1 trafficking and membrane insertion of Ca2+ permeable AMPA receptors in dorsal horn neurons is dependent on spinal tumor necrosis factor, PI3 kinase and protein kinase A [J]. Exp Neurol, 2017, 293: 144-58.

[34] GIACCO V, PANATTONI G, MEDELIN M, et al. Cytokine inflammatory threat, but not LPS one, shortens GABAergic synaptic currents in the mouse spinal cord organotypic cultures [J]. J Neuroinflammation, 2019, 16(1): 127.

[35] DODDS K N, BECKETT E A, EVANS S F, et al. Glial contributions to visceral pain: implications for disease etiology and the female predominance of persistent pain [J]. Transl Psychiatry, 2016, 6(9): e888.

[36] ESPINOZA K, SCHALER A W, GRAY D T, et al. Dynamic changes in mitochondria support phenotypic flexibility of microglia [J]. Nat Commun, 2025, 16(1): 11103.

[37] LI Y, XIA X, WANG Y, et al. Mitochondrial dysfunction in microglia: a novel perspective for pathogenesis of Alzheimer's disease [J]. J Neuroinflammation, 2022, 19(1): 248.

[38] ZENG H, WANG B, HUANG Z, et al. FOXA2 regulated by HDAC3-mediated deacetylation attenuates neuropathic pain by modulating microglial lipid metabolism and synaptic pruning dysregulation [J]. J Neuroinflammation, 2025, 22(1): 280.

[39] SHAO S, XU C B, CHEN C J, et al. Divanillyl sulfone suppresses NLRP3 inflammasome activation via inducing mitophagy to ameliorate chronic neuropathic pain in mice [J]. J Neuroinflammation, 2021, 18(1): 142.

[40] DEUS C M, TAVARES H, BEATRIZ M, et al. Mitochondrial Damage-Associated

Molecular Patterns Content in Extracellular Vesicles Promotes Early Inflammation in Neurodegenerative Disorders [J]. Cells, 2022, 11(15).

[41] SCHEIBLICH H, EIKENS F, WISCHHOF L, et al. Microglia rescue neurons from aggregate-induced neuronal dysfunction and death through tunneling nanotubes [J]. Neuron, 2024.

[42] CHEN W, LUO C, ZHOU H, et al. Mitophagy-mtROS axis contributes to anti-tuberculosis-induced liver injury through activation of the cGAS-STING pathway in rat hepatocytes [J]. Int Immunopharmacol, 2025, 160: 114984.

[43] ZHAO M, WANG Y, LI L, et al. Mitochondrial ROS promote mitochondrial dysfunction and inflammation in ischemic acute kidney injury by disrupting TFAM-mediated mtDNA maintenance [J]. Theranostics, 2021, 11(4): 1845-63.

[44] PERUZZOTTI-JAMETTI L, WILLIS C M, KRZAK G, et al. Mitochondrial complex I activity in microglia sustains neuroinflammation [J]. Nature, 2024.

[45] ZOROV D B, JUHASZOVA M, SOLLOTT S J. Mitochondrial reactive oxygen species (ROS) and ROS-induced ROS release [J]. Physiol Rev, 2014, 94(3): 909-50.

[46] HALESTRAP A P, RICHARDSON A P. The mitochondrial permeability transition: a current perspective on its identity and role in ischaemia/reperfusion injury [J]. J Mol Cell Cardiol, 2015, 78: 129-41.

[47] KOENIG A, BUSKIEWICZ-KOENIG I A. Redox Activation of Mitochondrial DAMPs and the Metabolic Consequences for Development of Autoimmunity [J]. Antioxid Redox Signal, 2022, 36(7-9): 441-61.

[48] HU M M, SHU H B. Mitochondrial DNA-triggered innate immune response: mechanisms and diseases [J]. Cell Mol Immunol, 2023, 20(12): 1403-12.

[49] WANG Y, XU X, JIANG G. Microplastics exposure promotes the proliferation of skin cancer cells but inhibits the growth of normal skin cells by regulating the inflammatory process [J]. Ecotoxicol Environ Saf, 2023, 267: 115636.

[50] ZHANG C Y, OU A J, JIN L, et al. Cadmium exposure triggers alveolar epithelial cell pyroptosis by inducing mitochondrial oxidative stress and activating the cGAS-STING pathway [J]. Cell Commun Signal, 2024, 22(1): 566.

[51] KIM J, KIM H S, CHUNG J H. Molecular mechanisms of mitochondrial DNA release and activation of the cGAS-STING pathway [J]. Exp Mol Med, 2023, 55(3): 510-9.

[52] DVORKIN S, CAMBIER S, VOLKMAN H E, et al. New frontiers in the cGAS-STING intracellular DNA-sensing pathway [J]. Immunity, 2024, 57(4): 718-30.

[53] HU Y, CHEN Y, LIU T, et al. The bidirectional roles of the cGAS-STING pathway in pain processing: Cellular and molecular mechanisms [J]. Biomed Pharmacother, 2023, 163: 114869.

[54] DONNELLY C R, JIANG C, ANDRIESSEN A S, et al. STING controls nociception via type I interferon signalling in sensory neurons [J]. Nature, 2021, 591(7849): 275-80.

[55] WU W, ZHANG X, WANG S, et al. Pharmacological inhibition of the cGAS-STING signaling pathway suppresses microglial M1-polarization in the spinal cord and attenuates neuropathic pain [J]. Neuropharmacology, 2022, 217: 109206.

[56] YANG M, KONG E, SONG H, et al. CMPK2 facilitates pain sensitization by promoting the lactylation and deactivation of cGAS-STING pathway in neuropathic pain [J]. Brain Behav Immun, 2025.

[57] ZHANG Y, WANG W, GONG Z, et al. Activation of the STING pathway induces peripheral sensitization via neuroinflammation in a rat model of bone cancer pain [J]. Inflamm Res, 2023, 72(1): 117-32.

[58] GAO R, MENG D, ZHAO Z, et al. VDAC1 Oligomerization-Mediated mtDNA Release under Sublethal Oxidative Stress: A Novel Inflammatory Mechanism in Vitiligo [J]. Free Radic Biol Med, 2025.

[59] JING Y, ZHANG Y, KADIER T, et al. Mitochondrial DNA release via mPTP and BAX/BAK drives inflammatory injury in intestinal ischemia reperfusion [J]. Cell Commun Signal, 2025.

8. Acknowledgements

We are grateful for Professor Tianjiao Xia's guidance on the pain behavioral testing in this experiment.

9. Funding

This study was supported by grants from the National Natural Science Foun dation of China (No. 82301405).

10. Ethics declarations

10.1 Ethics approval

All animal experiments were carried out in accordance with the protocols approved by the Laboratory Animal Ethics Committee of Nanjing Drum Tower Hospital (Approval number DWSY-23106410).

10.2 Consent for publication

All authors reviewed and approved the final manuscript for publication.

10.3 Competing interests

The authors declare no competing interests.

11. Authors' contributions

Study design: YLH, WZ, XPG. Data collection: HQT, XJS, MLC. Data analysis:HQT,MLC, RX. Manuscript preparation: HQT, XJS. Manuscript inspection:YLH, WZ, XPG. All authors read and approved the final manuscript.

12. Availability of data and materials

All data generated or analyzed during this study are included in this published article.